Proceedings of the ASME 2015 International Design Engineering Technical Conference & Computers and Information in Engineering Conference
IDETC/CIE 2015
August 2-5, 2015, Boston, Massachusetts, USA

DETC2015-47593

DRAFT: IDENTIFICATION OF HYDRAULIC BUSHING NONLINEAR DYNAMIC PROPERTIES

Tan Chai
Southern Illinois University
Carbondale, IL, USA

Jason T. Dreyer
The Ohio State University
Columbus, OH, USA

Rajendra Singh
The Ohio State University
Columbus, OH, USA

ABSTRACT

Hydraulic bushings are widely employed in vehicle suspension and sub-frame systems to control motion, and isolate noise and vibration. Although such devices exhibit significant excitation-profile-dependent dynamic properties, prior literature mainly focused on linear system analyses. Thus, this article examines the nonlinear characteristics of common hydraulic bushing configurations. First, a nonlinear model for a bushing with long and short passages in parallel is developed using a lumped parameter approach. Then the system parameters and nonlinearities of a laboratory prototype are identified using experiments and finite element tools, with an emphasis on the characterization of the flow passages. Steady state harmonic and transient step experiments are conducted on the prototype, and the pressures inside two fluid chambers and the force transmitted to the base are measured. Solutions of the nonlinear model show that the proposed model can well predict both steady state sinusoidal and transient responses for either single or multi-passage configurations.

INTRODUCTION

A typical hydraulic bushing usually consists of inner and outer metal sleeves, a rubber element, and two hydraulic chambers filled with anti-freeze and water mixture [1-6]. The two chambers are usually connected by one or more flow passages which communicate fluid between two chambers when a relative deflection of the inner and outer metal sleeves causes pressures to vary. Although hydraulic bushings exhibit significant frequency-dependent and amplitude-sensitive properties, prior articles essentially employed linear system theory to examine their spectral characteristics [1-5]. Therefore, specific objectives of this paper are as follows: (1) Formulate the nonlinear model of common fluid-filled bushing configurations, and identify fluid passage nonlinearities via experiments on a laboratory prototype; and (2) Validate the nonlinear model by comparing harmonic and transient response predictions with measurements.

NONLINEAR FLUID SYSTEM MODEL

The fluid model for a bushing with parallel long and short flow passages is developed in Fig. 1. The hydraulic elements are represented by several control volumes, and incompressible flow is assumed. Note that the internal long fluid passage (#*i*, the inertia track) is shown as external tubing for the sake of clarity. Static and dynamic displacement excitations are applied to the inner metal part while the outer metal sleeve is fixed relative to the inner sleeve. The rubber element (#*r*) is represented by a Kelvin-Voigt model with excitation displacement-dependent rubber stiffness $k_r(x)$ and viscous damping coefficient $c_r(x)$. The two fluid chambers (#1 and #2) are described by nonlinear compliance elements $C_1(p_1)$ and $C_2(p_2)$, respectively, with effective pumping areas A_1 and A_2. The fluid passages are represented by nonlinear fluid inertances $I_i(q_i)$ and $I_s(q_s)$ and nonlinear fluid resistances $R_i(q_i)$ and $R_s(q_s)$, respectively, where q is the volumetric flow rate. Note that R_i and R_s also include the minor momentum losses at the tube fittings and bends, etc. [7].

The dynamic displacement excitation $x(t)$, from the static equilibrium, is applied to the bushing (under a mean load f_m). By applying the momentum and continuity equations to each flow passage and two fluid chambers, the following equations are obtained:

$$p_1(t) - p_2(t) = I_i(q_i)\dot{q}_i(t) + R_i(q_i)q_i(t), \quad (1a)$$

$$p_1(t) - p_2(t) = I_s(q_s)\dot{q}_s(t) + R_s(q_s)q_s(t), \quad (1b)$$

$$-A_1\dot{x}(t) - q_i(t) - q_s(t) = C_1(p_1)\dot{p}_1(t), \quad (1c)$$

$$A_2\dot{x}(t) + q_i(t) + q_s(t) = C_2(p_2)\dot{p}_2(t). \quad (1d)$$

Here, $q_i(t)$ and $q_s(t)$ are the dynamic volumetric flow rates through long track and short passages, and $p_1(t)$ and $p_2(t)$ are the dynamic pressures inside the two fluid chambers, respectively. When only one passage is used, say a long inertia track, the governing equations for that configuration are obtained by setting $q_s(t) = 0$ and $R_s \to \infty$.

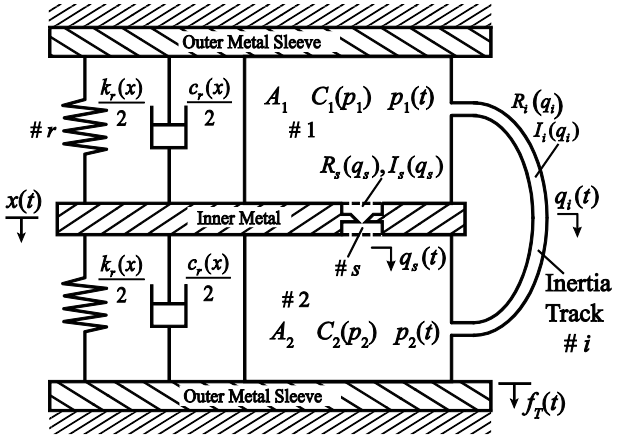

Figure 1. NONLINEAR FLUID SYSTEM MODEL OF A HYBRAULIC BUSHING.

With respect to the total dynamic force transmitted to the outer sleeve, $f_T(t)$ is divided into the rubber (subscript r) and hydraulic (subscript h) paths:

$$f_T(t) = f_m + f_{Tr}(t) + f_{Th}(t), \quad f_{Tr}(t) = k_r(x)x(t) + c_r(x)\dot{x}(t),$$
$$f_{Th}(t) = A_2 p_2(t) - A_1 p_1(t). \qquad \text{(2a-c)}$$

EXPERIMENTAL STUDIES

A laboratory device, as described in our prior article [4], is utilized to characterize bushing nonlinearities. This device consists of two similar chambers filled with water and a customized mid-plate which accommodates external long and short flow passages. To simulate typical real life fluid-filled bushing designs, three configurations of the prototype, as illustrated in Fig. 2 (a) to (c), are evaluated. First, configuration B1 is investigated when the two hydraulic chambers are connected by only one long passage. Second, B2 configuration is examined when the long passages are closed and the short passage orifice is fully open. Finally, the combination of long and short passages in parallel is examined by using B3 configuration; refer to [4] for more details.

The steady state sinusoidal experiments are first conducted on the above mentioned configurations using a non-resonant elastomer test machine (MTS 831.50, [8]). A sinusoidal displacement excitation $x(t) = A_x \sin 2\pi f t$ is applied to the prototype device under a mean load, where A_x is the zero to peak amplitude, and f is the excitation frequency (Hz). The transmitted force $f_T(t)$ and dynamic pressure inside two chambers, $p_1(t)$ and $p_2(t)$, are measured from 1 to 60 Hz with 1 Hz increment under two amplitudes, X = 0.1 and 1.0 mm, where $X = 2A_x$ is the peak to peak (p-p) value. Significant amplitude and frequency dependence is observed from the measured dynamic stiffness spectra for B1, B2, and B3 configurations with X = 0.1 and 1.0 mm.

Next, a step-up and step-down displacement excitation is also applied to the prototype device under a mean load. Measurements of transient responses imply that the dynamic responses highly depend on the step excitation amplitude. Accordingly, the nonlinear system parameters must be identified to model the excitation profile dependent properties.

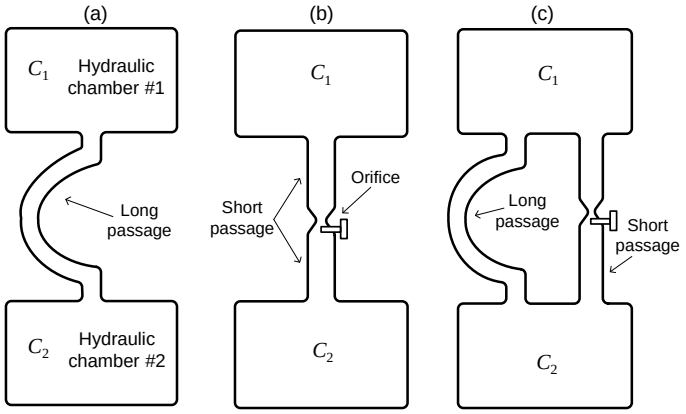

Figure 2. CONFIGURATIONS OF THE HYDRUALIC BUSHING CONSTRUCTED FOR LABORATORY STUDIES. (a) CONFIGURATION B1 WITH LONG FLUID PASSAGE OF DIAMETER d_i; (b) CONFIGURATION B2 WITH SHORT FLOW PASSAGE WITH RESTRICTION DIAMETER d_o; (c) CONFIGURATION B3 WITH PARALLEL LONG AND SHORT FLOW PASSAGES.

IDENTIFICATION OF SYSTEM PARAMETERS

The rubber path is approximated by the Kelvin-Voigt model, rubber stiffness and viscous damping elements k_r (ω, X) and $c_r(X)$ are estimated by interpolating measured dynamic stiffness of a bushing with fluid drained.

In order to estimate C_1 or C_2, a laboratory experiment is carried out to measure a change in chamber internal volume (ΔV) due to an incremental pressure (Δp). Then the fluid compliance around an operating point (o) is estimated as $C \approx \Delta V/\Delta p|_o$. It is observed from measured ΔV vs. Δp data that as the pressure is increased from 0 to around 180 kPa, $\Delta V/\Delta p$ variation is less than 15%. Therefore, C_1 and C_2 are assumed to be linear, and their values are estimated based on a linear polynomial fit of measurements. The effective pumping areas $A_{1,2}$ are examined next by employing a structural finite element code. Results show that a variation of $A_{1,2}$ is less than 3% when the load is varied from 100 to 1000 N. Thus, $A_{1,2}$ values are also assumed to be constant.

Inertance of long and short passages is calculated as $I_i = \rho l_i/A_i$ and $I_s = \rho l_s/A_s$ by assuming unsteady turbulent flow [9].

A bench experiment is conducted to measure the steady flow rate (q) through each fluid passage under a pressure differential (Δp, range from 6.9 to 206.8 kPa). Experimental

results show that the Δp to q relationship is nonlinear for each passage. Accordingly, the nonlinear resistance ($R_i(q_i)$) of a long passage is defined based on a fully developed turbulent flow in a smooth circular pipe [7] as:

$$R_i(q_i) = \frac{\Delta p}{q_i} = \lambda_i \frac{0.242 l_i \mu^{0.25} \rho^{0.75}}{d_i^{4.75}} q_i^{0.75}. \quad (3)$$

Here, an empirical scaling factor $\lambda_i \approx 1.4$ is employed to account for momentum losses at the tube bends and fittings, and ρ and μ are the water density and viscosity, respectively.

The nonlinear resistance $R_s(q_s)$ for a short passage of effective diameter d_o is defined by using the well known orifice formula [7] with an empirical factor λ_s:

$$R_s(q_s) = \lambda_s \frac{\rho}{2C_d^2 A_o^2} |q_s|. \quad (4)$$

Here, C_d is the discharge coefficient and $A_o = \pi d_o^2/4$ is the geometric cross-sectional area.

EXPERIMENTAL VALIDATION OF NONLINEAR MODEL

Based on the identified system parameters, this nonlinear model is numerically solved using an explicit 4th and 5th order Runge-Kutta method. The steady state harmonic responses predicted by the nonlinear model are compared with measured pressure and transmitted force. Excellent agreement between the nonlinear model and measurements are observed for both low and high excitation amplitudes. For example, the predicted steady harmonic responses of B2 under 10 Hz excitation, as shown in Fig. 3, provides an excellent agreement with measurements at both X = 0.1 and 1.0 mm, especially for the super-harmonic terms.

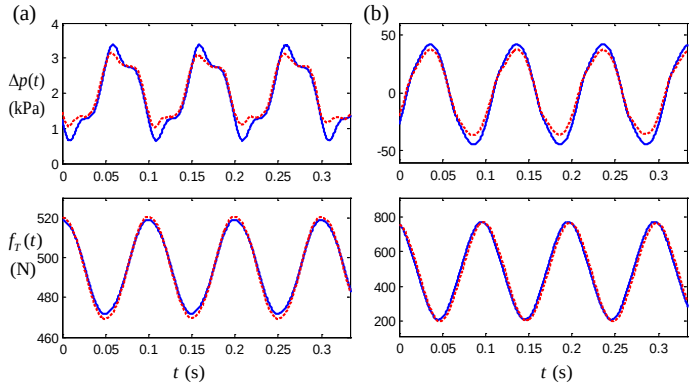

Figure 3. COMPARISON OF NONLINEAR MODEL PREDICTIONS AND MEASUREMENTS FOR HARMONIC RESPONSES OF CONFIGURATION B2 AT 10 HZ. (a) X = 0.1 mm; (b) X = 1.0 mm. KEY: ——, NONLINEAR MODEL; – – –, MEASUREMENTS.

The nonlinear model predictions of the step-up and step-down responses of B1 are compared in Fig. 4 with transmitted force measurements. Predicted $f_T(t)$ matches well with measured forces as shown in Fig. 4. Likewise, an excellent agreement is observed for both step-up and step-down responses of B2 and B3. These comparisons confirm that the nonlinear model represents the nonlinearities well in the transient responses for both single and dual-passage bushing configurations.

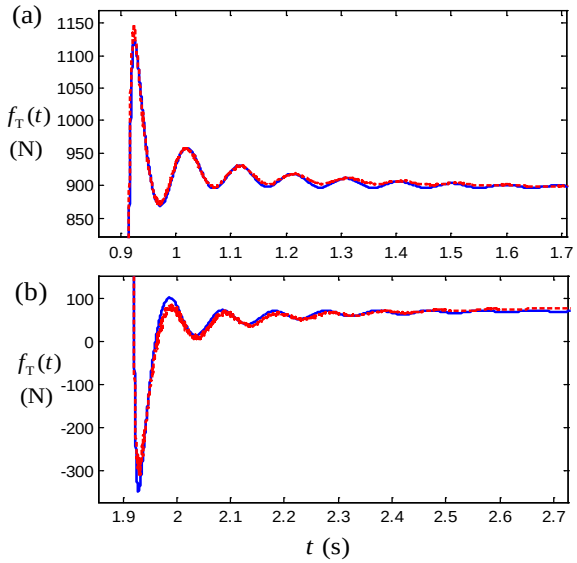

Figure 4. COMPARISON OF PREDICTED AND MEASURED TRANSIENT RESPONSES FOR CONFIGURATION B1. (a) STEP-UP RESPONSE WITH STEP EXCITATION AMPLITUDE $A_e = A_{xt}$; (b) STEP-DOWN RESPONSE WITH $A_e = 2A_{xt}$. KEY: ——, NONLINEAR MODEL; – – –, MEASUREMENTS.

CONCLUSION

This study has developed a refined nonlinear model for a bushing with long and short passages and identified key nonlinear parameters using theory and experiment. The system nonlinearities are found to be dominated by the fluid resistance terms and thus these are defined based on the turbulent flow formulation. By using the nonlinear model, three configurations of the laboratory prototype device are examined. The nonlinear model is solved by using the numerical integration method, and its predictions match well with both steady state harmonic and transient measurements for either single or multi-passage configurations. Such nonlinear models should lead to better industrial design and tuning processes.

ACKNOWLEDGMENTS

We acknowledge the member organizations such as Transportation Research Center Inc., Honda R&D Americas, Inc., and YUSA Corporation of the Smart Vehicle Concepts Center (www.SmartVehicleCenter.org) and the National Science Foundation Industry/University Cooperative Research Centers program (www.nsf.gov/eng/iip/iucrc) for supporting this work. We also thank C. Gagliano and P. C. Detty for their help with experimental studies.

REFERENCES

1. Sauer, W., and Guy, Y., 2003, "Hydro bushings - innovative NVH solutions in chassis technology," SAE Paper 2003-01-1475,.
2. Piquet, B., Maas, C., and Capou, F., 2007, "Next generation of suspension bushings: reviews of current technologies and expansion upon new 3rd generation product data," SAE Paper 2007-01-0850.
3. Lu, M., and Ari-Gur, J., 2000, "Study of dynamic properties of automotive hydrobushing," *ASME Design Engineering Division Proceedings*; *Vol. 106*, pp. 135-140.
4. Chai, T., Dreyer, J. T., and Singh, R., 2015, "Frequency domain properties of hydraulic bushing with long and short passages: System identification using theory and experiment," *Mechanical Systems and Signal Processing*, *Vol. 56-57*, pp. 92-108.
5. Chai, T., Dreyer, J. T., and Singh, R., 2013, "Time domain responses of hydraulic bushing with two flow passages," *Journal of Sound Vibration*, *Vol. 333*, pp. 693-710.
6. Chai, T., Dreyer, J. T., and Singh, R., 2015, "Nonlinear dynamic analysis of hydraulic suspension bushing with emphasis on flow passage characteristics," *Proc IMechE Part D: J. Automobile Engineering*, DOI: 10.1177/0954407014561048.
7. Merritt, H. E., 1967, *Hydraulic Control Systems*. New York: John Wiley & Sons.
8. MTS Elastomer Test System Model 831.50 (1000 Hz), at http://www.mts.com.
9. Doebelin, E. O., 1998, *System Dynamics: Modeling, Analysis, Simulation, Design*. New York: Marcel Dekker.